*35th EPS Conference on Plasma Phys. Hersonissos, 9 - 13 June 2008 ECA Vol.**32D**, P-5.088 (2008)*

Interaction of ITER-like ICRF antenna with Tore Supra plasmas: insight from modelling.

A. Mendes[1], L. Colas[1], A. Argouarch[1], S. Brémond[1], F. Clairet[1], C. Desgranges[1], A. Ekedahl[1], G. Lombard[1], D. Milanesio[2], L. Millon[1], P. Mollard[1], D. Volpe[1], K. Vulliez[1].

[1]CEA-IRFM, F-13108 St. Paul-lez-Durance, France
[2]Department of Electronics, Politecnico di Torino, Turin, Italy

The non-linear interaction of ion cyclotron resonance frequency (ICRF) waves with the plasma edge is one of the challenges faced by high power wave heating systems in next step devices. Such interaction is often associated with parallel RF electric fields excited by spurious parallel RF currents flowing on the antenna front face [1]. One way to test this conjecture is to investigate how RF-induced edge perturbations develop spatially around ICRF launchers, for a large variety of RF current flows [1]. In 2007 a novel ICRF ITER-like (IL) antenna was tested on the TS tokamak, offering hence the unique opportunity to document wave-plasma interactions in the tokamak edge, on the same target plasmas as classical antennae, but with different patterns of RF currents on the antenna front face and different points of high RF voltage, thus imposing tighter constraints on interpretative physics models. The present paper confronts theoretical models with selected experimental results and suggests ways to decrease the wave-plasma interaction for a recessed antenna.

I – Experimental results

1 ´ ICRF antenna configurations. The prototype launcher (Fig 1´ a) is composed of two ITER-like (IL) circuits arranged toroïdally. Each IL circuit is composed of two poloïdal current straps short circuited on one side on the Faraday Screen (FS) and connected in series to variable capacitors at the other one. Compared to the classical antenna (Fig 1´ b), the strap´FS distance was increased on IL antenna, a large septum was introduced and the high voltage point (in the sense of transmission line theory, $V_{StripLine}$ on Fig. 1´b) is now closer to the equatorial plane. Both launchers feature plug-in structures protruding ~8cm in front of the vacuum vessel wall.

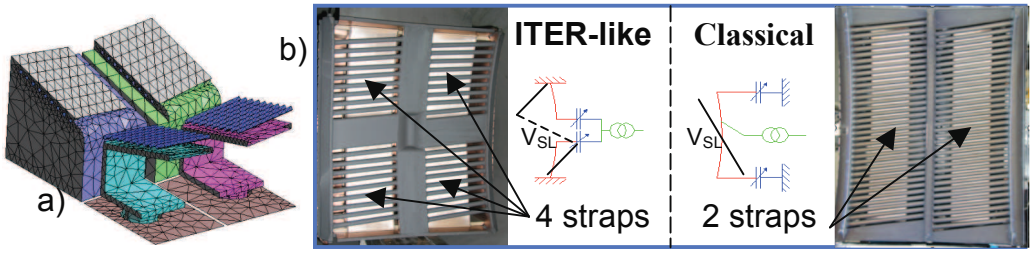

Figure 1: (a), antenna modelling with triangular mesh of 3D surface used for the simulation. (b), ITER-like vs. classical antenna with their electric scheme.

2 ´ Coupling resistance. The antenna ability to convey RF power to the plasma is characterized by a *coupling resistance,* R_c (in $\Omega.m^{-1}$). On Tore Supra, R_c is calculated from an electrical model of the IL circuit, using measurents of power transmitted to the plasma and RF voltage measurement near capacitors. For both antennae, figure 3 exhibits a correlation of R_c with the distance, d_{sco}, between the strap and a characteristic density *cut-off* layer (for $k_{//}=14m^{-1}$ in the launched spectrum) beyond which the *fast wave* becomes propagative [2]. The strap´cut-off distance is determined experimentally from edge density profiles using X-mode reflectometry. d_{sco} was changed dynamically either by moving the plasma radially, or by supersonic gas injections. By fitting the two distributions we exhibit the curve slope in logarithmic scale, related to the fast wave evanescence at the maximum $k_{//}$ of the antennae spectrum. Moreover, R_c is slightly higher in the classical case.

3 ´ Experimental evidence of localized RF-induced density modifications.

All plasma facing components on Tore Supra are monitored by infrared thermography [3]. As shown on fig. 2´a the surface temperature increases on the ICRF antenna front face, and this only when it is powered. In spite of the launcher geometrical symmetry, the observed heat loads are asymmetric, namely higher in the top-left antenna box corner than in bottom-right one. This asymmetry, already observed on classical antenna, was explained by a local density influx induced by HF [1] as discussed later. The hot spot locations are NOT affected by the change of high voltage point. The hottest zone is now located near RF ground.

The four waveguide rows of a neighbouring Lower Hybrid (LH) wave launcher are magnetically connected to the IL antenna at different poloïdal positions near its lower right box corner. Fig. 2´b shows that when the ICRF prototype is energized, both the LH coupling properties and the heat loads on the LH launcher evolve differently on the four rows. Similar behaviour was also observed for similar magnetic connections from LH launcher to the classical antenna and was attributed to inhomogeneous RF-induced density modifications in the lower part of the ICRF antenna [4].

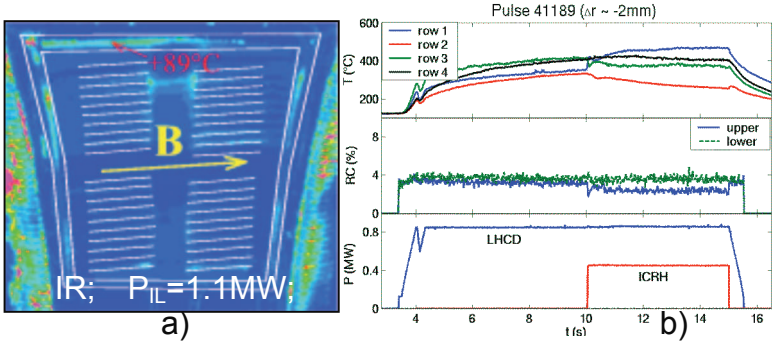

Figure 2: (a), infrared view of powered ITER-like antenna during plasma. Superimposed: sketch of front face structure. (b), LH launcher behaviour during combined ICRF+ LHCD pulse. Time traces of LH power reflection coefficients and IR surface temperatures on four waveguide rows numbered from top to bottom.

II – Antenna simulation

1 ´ Simulation setup. The IL antenna has been simulated with antenna code TOPICA [3] and a hot plasma model obtained in the present case with FELICE code [4]. The electrical model, depicted on figure 1´a, consists of 4 cavities, each one containing one strap and a coaxial cable as feeder. By construction the four cavities are recessed in a metallic wall and radiate to the plasma though an aperture (meshed by 98 triangles, visible on figures 1, 4). For near field computations the feeding RF voltages were tuned to 1V in amplitude, π-toroïdal phasing and 0-poloidal phasing. Field line pitch angle was 7° (see fig. 4).

2 ´ R_c comparison. The coupling resistance R_c averaged over the four straps is obtained from the simulated 4×4 impedance matrix Z from formula:

$$R_c = \mathrm{Re}\left(\sum_{a,b} Z_{a,b} \cdot e^{i(\varphi_b - \varphi_a)}\right) \cdot \frac{1}{4L}$$ where L is the strap length and φ_a, φ_b are the phases of the feeding tensions.

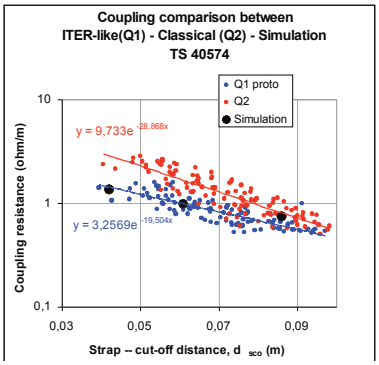

For this comparison, three experimental plasma profiles from the same shot have been introduced in FELICE, essentially different by their distances strap´ cut-off. Figure 3 presents the good agreement between the simulation and experimental data (blue dots). The shape difference between IL and classical experimental data is attributed to the poor statistics but need to be confirmed with more data shot and also by simulation.

Figure 3: Comparison of R_c, as a function of distance strap¨ cut-off, between 3 simulated plasmas (black) and experimental data (red for IL, blue for classical antenna).

3 ´ RF Electric field map on antenna aperture. Presently, the radiated parallel RF electric field, shown in Fig. 4, has been computed on the radial plane containing the antenna aperture. Three expected results are observed: first the RF field emerges from the aperture in the metallic wall and is 0 everywhere else; secondly, the π-toroïdal phasing can be seen from the sign of $E_{//}$ on neighbouring straps; finally the electric field $E_{//}$ (~E_{toro}) exhibits opposite signs on the two toroïdal sides of each strap, consistently with strip line theory. The fine-scale discretization of the RF field map is related to the meshing of the aperture.

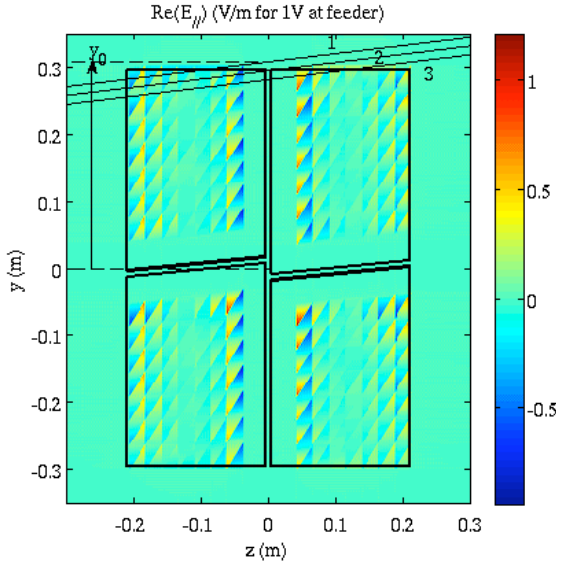

Figure 4: 2D (toroïdal poloïdal) electric field map for $E_{//}$ on the aperture. The antenna box is drawn with black lines together with 3 selected field lines and the definition of y_0 (see figure 5).

III – RF sheath modelling

1 ´ Principle. Several theoretical models predict RF-enhanced DC sheath potentials [5, 6]. Within the simplest model [5], ICRF antenna operation drives a pure RF oscillating potential ΔV_{RF} between the extremities of open magnetic flux tubes (supposed independent), given by $\Delta V_{RF} = \int_L \mathbf{E}_{//}.\mathbf{dl}$ where $\mathbf{E}_{//}$ is the RF parallel electric field, and integration is performed along the open field lines (see figure 4).

In this model with independent flux tubes, each field line develops its own DC potential. Since the mapping of ΔV_{RF} is spatially inhomogeneous, the differential biasing of nearby flux tubes creates DC $\mathbf{E_{DC}}\times\mathbf{B_0}$ particles convection transversally to the field lines [7]. It was shown that $\mathbf{E_{DC}}\times\mathbf{B_0}$ convection could create an up and down density unbalance in the vicinity of classical TS antennae, and hence an asymmetrical hot spot pattern. Below we will focus on the geometry of the ΔV_{RF} around powered IL antenna.

2 ´ Results and discussion. ΔV_{RF} was obtained by numerical integration of $E_{//}$ along tilted straight lines (see fig. 4). The discretization of $E_{//}$ has probably a limited impact on V_{RF}, since it is a line-integrated quantity. Fig. 5´a plots poloïdal profiles of $Re(\Delta V_{RF})$ for the IL antenna (black) and two antennae derived from the latter, using the intermediate plasma of fig. 3 as load. Several substructures are visible: ´double peaks´ at top and bottom, meaning that box corners are favourable with the appearance of high potential; a middle part with null potential, surrounded by two small ´single peaks´. These peaks do not evolve when the mesh is refined on the apertures, while all the other contributions decrease in amplitude.

´Double peaks´ are actually two peaks with approximately the same amplitude but opposite signs. Their large amplitude is attributed to adverse current circulation in the corners and is in addition worsened by the tilt angle between the box and the magnetic field line at top and bottom part only (as pictured with the 3 field lines on figures 4-5). The sign difference is probably due to an opposite current circulation along the right and left part of the box. This clearly means that a ´parallelogram box´, as the blue and red examples (Fig. 5´a), with edges aligned with tilted magnetic field lines, would drastically cancel these top and bottom high potential, since the two peaks would in that case annihilate each other. This is confirmed numerically on Fig. 5´a.

The ´double peaks´ are probably linked to the recessed antenna structure inherent to TOPICA. Indeed, Fig. 5´b plot still shows ΔV_{RF} but here obtained with a protruding antenna structure closer to TS situation (but without FS), using the ICANT simulation code [8]. The protruding antenna develops a single peak in front of the box frame, that broadens poloïdally and decreases in amplitude as the frame height is increased to approximate a recess. Via RF sheath rectification and $\mathbf{E_{DC}}\times\mathbf{B}$ convection, the peaks in figure 5´b are likely to explain localised density modifications in the upper and lower parts of the IL antenna, as suspected from the observations with IR thermography and LH coupler.

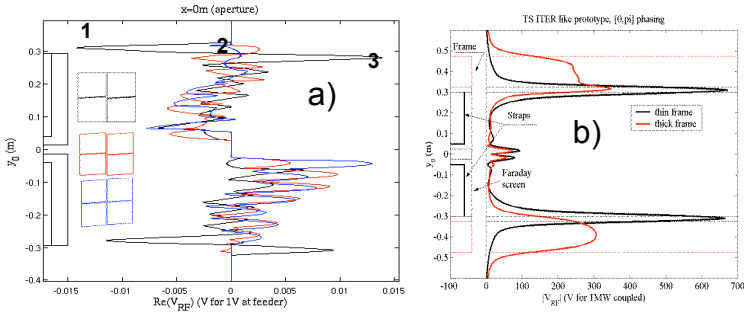

<u>Figure 5</u>: Re(ΔV_{RF}) (a) for 3 different antennae. ΔV_{RF} is evaluated at the antenna aperture, and is plotted versus the altitude y_0 where tilted field lines intersect the antenna mid-plane (see fig. 4). Points (1)-(3) correspond to field lines numbered on fig. 4. (b), $|\Delta V_{RF}|$ for protruding IL launcher, comparing thin and thick frames (see sketches, both on left side).

IV – Conclusion

When the maximum RF voltage of strip line theory is displaced towards equatorial plane compare to a classical antenna, the fast wave coupling with plasma is reduced on the IL launching structure. Further investigation is needed to explain the differences, ranging from 22% to 50%. Localised SOL modifications are suspected in the upper and lower parts of the IL antenna. These indications still need to be corroborated with spatially resolved reciprocating probe measurements. Observations are consistent with poloïdal profiles of ΔV_{RF} obtained with a protruding antenna box. This stresses the adverse role of parallel currents on the box frame and nearby FS rods on RF sheath generation. The effect of the nearby wall and of the grounding scheme on the near field patterns needs to be further clarified to make reliable predictions for e.g. ITER. In order to use TOPICA to compute realistic RF fields for a protruding antennae like Tore Supra, it might be necessary to include the launching structure in a large recess. A recessed antenna, coupled with a parallelogram box design seems to be an efficient option to suppress the corner effect both for IL or classical schemes with π phasing.

Acknowledgements

This work, supported by the European Communities under the contract of Association between EURATOM and CEA, was carried out within the framework of the European Fusion Development Agreement. The views and opinions expressed herein do not necessarily reflect those of European Commission.

References

[1] L. Colas, Nucl. Fusion **45** (2005), 767-782.
[2] F. Clairet *et al*, Plasma Phys. Control. Fusion **46** (2004) 1567-1580.
[3] D. Guilhem *et al*, Fusion Eng. Design, **74** (2005), 879.
[4] L. Colas *et al*, Plasma Phys. Control. Fusion **49** (2007) B35-B45.
[5] V. Lancelloti *et al*, Nucl. Fusion **46** (2006), S476-S499.
[6] M. Brambilla, Plasma Phys. Control. Fusion **31** (1989), 723.
[7] F. W. Perkins, Nucl. Fusion **29** (1989), 523.
[8] D.A. D´Ippolito and J.R. Myra, Phys. Plasma **13** (2006), 102508.
[9] D.A. D´Ippolito *et al*, Phys. Fluids B **5** (1993), 3603.
[10] S. Pécoul *et al*, Comput. Phys. Commun. **146** (2000), 166-87.